JOURNAL OF MATERIALS SCIENCE 30 (1995) 339–346

Study of the Ti/Al_2O_3 interface

HUA LU, C. L. BAO, D. H. SHEN, X. J. ZHANG, Y. D. CUI, Z. D. LIN
State Key Laboratory for Surface Physics, Institute of Physics, Academia Sinica, P.O. Box 603, Beijing 100080, People's Republic of China

The Ti/Al_2O_3 $(1\bar{1}02)$ interface formation has been investigated by X-ray photoelectron spectroscopy and Auger electron spectroscopy (AES). The results showed that when an active metal titanium was evaporated on to a room-temperature Al_2O_3 $(1\bar{1}02)$ surface in ultrahigh vaccum, a Ti/Al_2O_3 interface region of about 200 nm was formed, and in the first several monolayers of titanium, the titanium was oxidized due to the active oxygen anions on the surface. Therefore, the pure Ti/Al_2O_3 interface was replaced gradually by a titanium oxides/Al_2O_3 interface, which has a stronger interaction than the former. The change of shape of the photoemission lines and the shift of binding energy of aluminium, oxygen and titanium with increasing coverage of titanium showed that the formation of the Ti–O bond at the interface is due to titanium transferring its electrons to Al^{3+} via O^{2-} anions in the Al–O bond, whereby the Al^{3+} was reduced to metallic aluminium, Al^0. The AES intensity profile also proved the existence of the reduced species Al^0. This suggests that the reaction layer consists of a multiphasic mixture: the Ti–O type phase, the $(Ti, Al)_2O_3$ phase and metallic aluminium phase.

1. Introduction

Metal/ceramic interfaces play a very important role in various aspects of electronic industries, including microelectronic packaging [1], thin-film devices [2] and the joining of structural ceramics with metals [3]. However, the physical process of the interface formation and the microscopic mechanism of bonding across an interface of a predominantly covalently bonded ceramic to a metal, are still not completely understood. Therefore, a knowledge of electronic structure and energy state of the metal/ceramic interfaces is needed for a better understanding of the interface, which could lead to adhesion improvement and bond strengthening, and dictate the properties of the component. As a substrate material, Al_2O_3 is widely used for ceramic packages, because of its good insulating properties, thermal and mechanical characteristics, and its chemical inertia. However, it requires a very strong adherence between the metallized layer and the substrate during integrated circuit (IC) packaging, especially when metallurgical attack occurs during the IC-chip attachment process. Therefore, a chemically active metal, titanium, was chosen as the metallized layer and deposited on a surface of the single-crystal Al_2O_3 (sapphire) for the formation of the interface. The thin film of pure titanium has the hcp structure, the same as that of the sapphire, and the thermal expansion coefficient of titanium is also analogous to the sapphire, therefore, a tendency for epitaxial growth on the substrate surface is expected at a certain temperature range. We thus believe that this Ti/Al_2O_3 system can provide a model for many important interfaces and allow application of a number of techniques to the interface characterization. In previous experimental studies of metal/ceramic interfaces, some works [4–12] have been performed on the chemistry of the Ti/Al_2O_3 interface, and much valuable information has been obtained. In this paper, we will describe first the process of the interface formation. i.e. how the titanium atoms bind to the $(1\bar{1}02)$ plane of the sapphire, then discuss some new features of the Ti/Al_2O_3 interface investigated by X-ray photoemission spectroscopy (XPS) and Auger electron spectroscopy (AES).

2. Experimental procedure

The X-ray photoelectron spectrum was recorded by an ESCALAB MK-II spectrometer of VG Scientific Ltd. The system consists of two separately pumped chambers. The main analysis chamber is equipped with a non-monochromatized twin anode (aluminium and magnesium) radiation X-ray source with a microspot facility (from 150–1000 μm diameter), a hemispherical analyser and a flood gun for charge neutralization. The achieved resolution of the spectrometer was 1.1 eV with a pass energy of 20 eV, and the spectra were collected with a photoelectron emission angle 51.5° from the sample normal. The AES experiment was performed on a Perkin–Elmer Model PHI-610 Scanning Auger Microprobe with single-pass cylindrical mirror analyser (CMA) and coaxial electron gun ($0 < E_g < 10$ KeV); the focused electron beam (3 μm^2) can be scanned over the sample to obtain a secondary electron image of the sample. AES spectra were collected digitally in the $N(E)$ form and electronically differentiated. Data were analysed in the differentiated form, $dN(E)/dE$. Depth profiling was

0022–2461

performed with 2.0 kV Ar^+ ions incident at about 45° with respect to the sample normals, by alternately acquiring data and sputtering. The sample was a thin square slice of single-crystal Al_2O_3 (sapphire) with one face polished optically on the $(1\bar{1}02)$ plane using a diamond-tipped scribe. Samples were cut to approximately $10 \times 10\ mm^2$ for XPS and AES experiments. The samples were ultrasonically cleaned in trichloroethylene, acetone and ethanol, and then dipped in a concentrated solution of HF for 30 s for chemical etching. Finally, they were rinsed in pure H_2O, blown dry with highly pure nitrogen, and then mounted on a sample holder. In the case of the XPS experiment, the cleaned sample was immediately loaded into the pretreatment chamber of the XPS spectrometer next to the analysis chamber by a fast-entry airlock; in this chamber a vacuum of 10^{-10} torr (1 torr = 133.322 Pa) was maintained throughout the experiment. The sample must be further cleaned using an argon ion gun and/or flash-heating (750 °C heated by passing a current of up to 10 A through a tantalum sheet for only a few minutes in the order of 10^{-10} torr in order to eliminate the contaminants and to avoid both outgassing of the sample holder and decomposition of Al_2O_3) just prior to the deposition of titanium by physical vapour evaporation. Metallic titanium films were deposited on to a room temperature (RT) Al_2O_3 substrate in ultrahigh vacuum (UHV) by evaporating ultra-pure titanium wires from a tungsten filament (tungsten basket) through resistive heating. The basket is predegassed in UHV for several hours until a base pressure of 10^{-10} torr is reached. This evaporation method allows one to obtain a very low rate less than $15\ nm\ min^{-1}$. Then, the metallized Al_2O_3 sample was transferred to the main chamber of the XPS spectrometer for XPS analysis. For all XPS experiments, MgK_α ($h\nu = 1253.6$ eV) radiation was used. The AES analysis of the clean surface of the sample and the Ti/Al_2O_3 $(1\bar{1}02)$ interface were accomplished after argon plasma sputter etching.

3. Results and discussion

3.1. Clean surface

Because of charging effect inherent in insulators, all XPS data have to be calibrated with reference to an available accurate optical data. We take an energy term, which is induced by the charging effect, into consideration in the original energy formula of the photoelectron emission. Thus, the kinetic energy of the photoelectrons may be expressed as

$$E_k = h\nu - E_B - \phi_{sp} - E_c \qquad (1)$$

where E_B is the binding energy of electrons with reference to the Fermi level, ϕ_{sp} is the work function of the spectrometer, and E_c is the energy induced by the charging effect, $E_c = V_s e$ (V_s is the surface potential, e is electronic charge). The charging effect could compel the XPS photoelectron lines to move towards the low kinetic energy side, and also could widen or distort the shape of the spectroscopic peaks; therefore, it could affect the analysis results if the energy, E_c, is not calibrated. Some XPS data, such as given in the literature [13], are referred to the C 1s line (binding energy, $E_B = 284.6$ eV) which is always present on the sample as a contaminant. In addition, the O1s line ($E_B = 531.6$ eV) can also be taken as the reference for the XPS data, as reported by Varma *et al.* [14]. These, however, are not constant, even for the same apparatus. Other methods include internal mixing of calibration substances and vacuum deposition of thin layers, e.g. gold. Their advantages and disadvantages are discussed in the literature [15, 16]. In our experiments, we take the XPS photoelectron line of elemental argon as a reference [17] for calibrating the E_c. Because argon is chemically inertial, its photoelectron line is created easily by bombardment of Ar^+ ions. The standard binding energy of the Ar $2P_{3/2}$, E_B, is equal to 241.3 eV. Our results showed that this method is very simple and available for the charging specimens. Fig. 1 shows the typical XPS core-level photoemission lines of the clean Al_2O_3 $(1\bar{1}02)$ plane. The surface is free from any carbon and other impurity contamination, but two small peaks of argon (Ar 2s, Ar 2p) embedded by Ar^+ ion bombardment can be observed clearly. AES data also showed that for an uncleaned Al_2O_3 $(1\bar{1}02)$ sample, carbon was the main contaminant. On sputtering the surface by Ar^+ ions for 10 min, the carbon signal was reduced to the noise level. The resulting spectrum is shown in Fig. 2. The spectral features of note are the minima at 36, 52 and 64 eV, respectively, due to Al (LVV) processes and those near 512 eV from the O (KVV) process. Except for the carbon contamination (near 271 eV), the spectra are identical before and after cleaning, and no changes were observed from the clean spectra with electron bombardment during these experiments. There is an accessible small argon signal (215 eV) that varied through the experiment without noticeable effect. In order to obtain the information on the chemical state of the clean surface, Al 2p and O 1s photoelectron lines were recorded. As shown in Fig. 3, Al 2p and O 1s feature lines appeared at 74.8 and 531.5 eV, respectively, which agree better with the energy values used in the Handbook [18]. Only one component appeared in the Al 2p photoelectron line, indicating the surface structure does not vary obviously after bombarding with Ar^+ ions. According to the suggestion by French and Somorjai [19], the surface reconstruction involves less oxygen, therefore if there was a removal of oxygen on the surface after irradiation by Ar^+ ions, there should be a noticeable additional signal in the Al 2p photoelectron line. But this was not observed. In order to follow the variation of the oxygen content at the surface, we calculated the ratio of the Al 2p to O 2s peak intensity from the XPS spectrum, with an uncertainty of $\sim 10\%$. As these two photoelectron energies were close to each other, the corresponding escape depths were expected to be of the same order. Therefore, it can be held to give a correct estimate of the aluminium to oxygen ratio at surface layers. Our measurement of the ratio of the intensity of the photoelectron lines Al (2p)/O(2s) ($= 3.0$) confirmed that the Al_2O_3 $(1\bar{1}02)$ plane is an aluminium-rich surface. This observation can be attributed to the fact that ion bombardment creates an oxygen deficiency at the sapphire surface. Moreover,

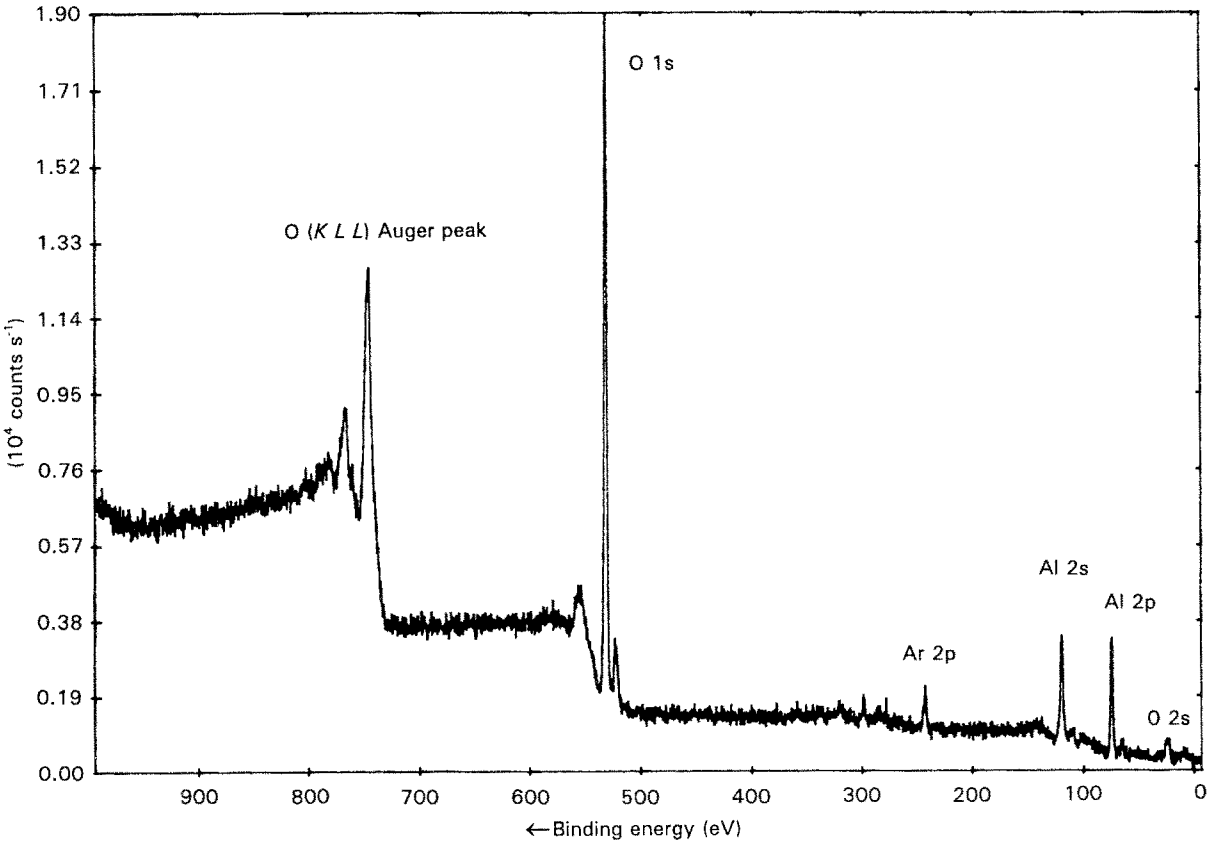

Figure 1 Typical XPS core-level photoemission lines of the clean Al_2O_3 ($1\bar{1}02$) surface collected with the non-monochromatized MgK_α X-ray source. The charging effect was calibrated with reference to the Ar2p line.

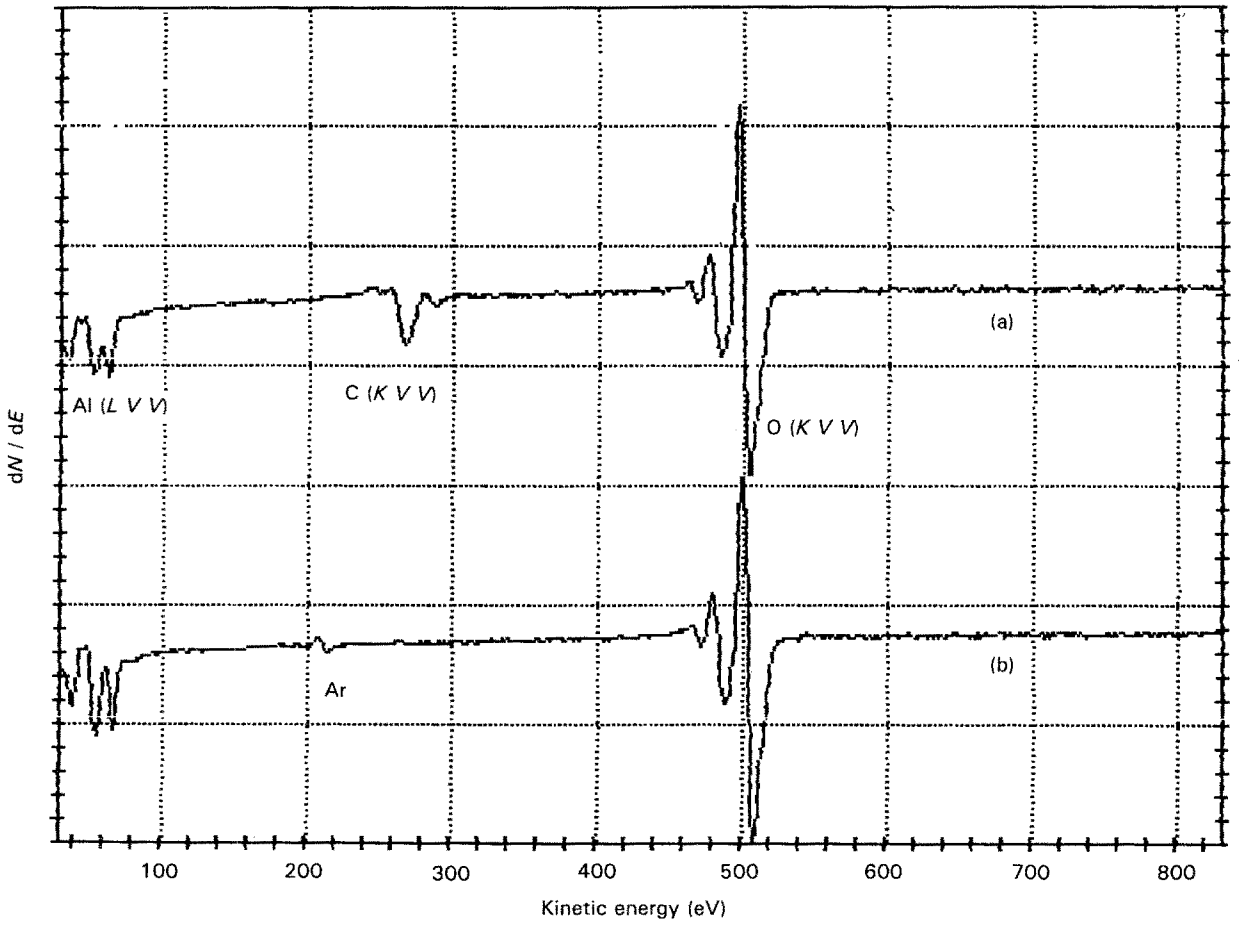

Figure 2 Auger electron spectrum of the Al_2O_3 ($1\bar{1}02$) surface, (a) before, and (b) after Ar^+ ion sputter cleaning.

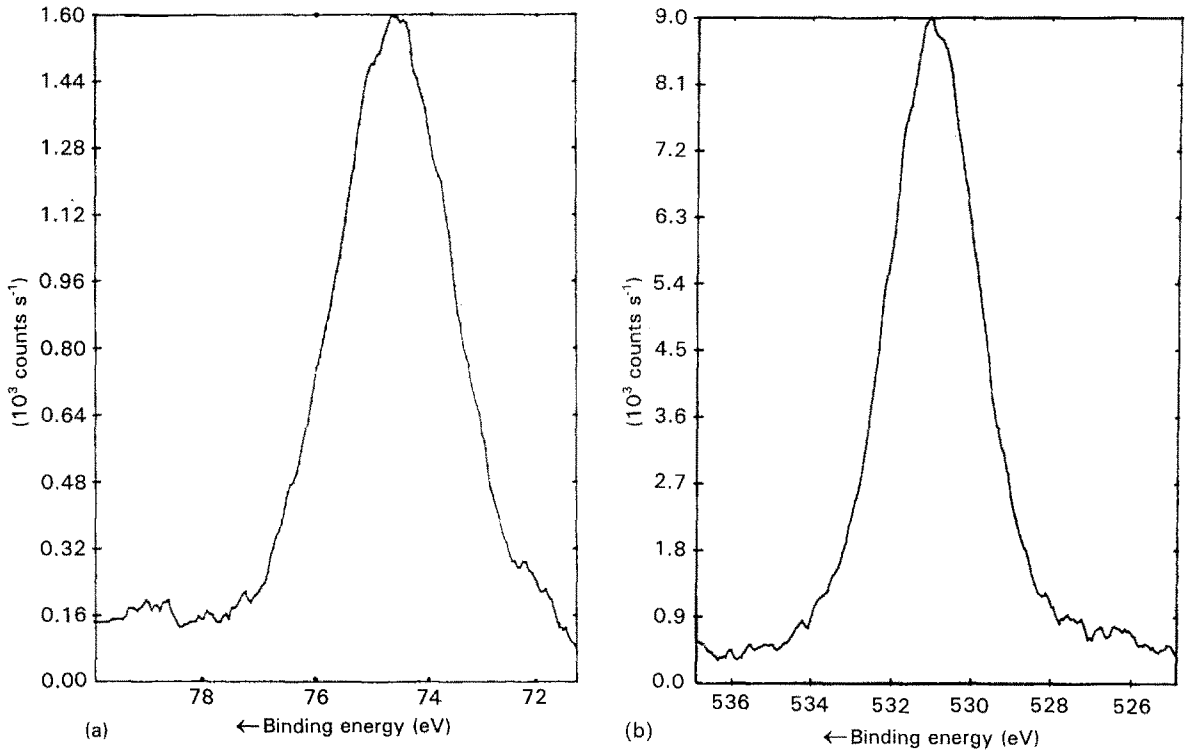

Figure 3 Photoelectron lines recorded using the non-monochromatized MgK_α X-ray source: (a) Al2p, and (b) O1s.

from the whole set of data, it can be inferred that the bombardment does not vary the surface structure, but only decreases the oxygen content by small amounts. Our XPS and AES results also demonstrated that the clean Al_2O_3 $(1\bar{1}02)$ surface is extremely stable and does not trap an appreciable amount of charge even during bombardment by the electron gun in AES measurement.

3.2. Ti/Al_2O_3 interface

After the XPS and AES experiments on the clean Al_2O_3 $(1\bar{1}02)$ plane were completed, titanium was evaporated on to the surface which was at room temperature, by physical vapour deposition. Single-crystal sapphire (Al_2O_3) has an hcp lattice ($a = 0.476$ nm, $c = 1.30$ nm) [20], and the number of atoms in a unit cell is 6. By calculation, therefore, we can define one monolayer (1 ML) of titanium on the Al_2O_3 $(1\bar{1}02)$ plane as the number of titanium atoms in a layer constituting the crystal itself, i.e. 9.1×10^{13} atoms cm^{-2}. The titanium film thickness was estimated from XPS intensity analysis [21–23]. For a uniformly thick film, the effective thickness, d, at the polar angle, α can be expressed as

$$d = \lambda_0 \sin\alpha \ln[1/R\,(I_0 I_s) + 1] \quad (2)$$

$$R = S_0 n_0 / S_s n_s \quad (3)$$

λ_0 is the inelastic mean free path of Ti2p photoelectrons in the adlayer which can be calculated using the empirical relationship quoted by Dreiling [24]:

$$\lambda_0 = 0.2\,E \times (\text{depth of a monolayer}) \quad (4)$$

where E is the kinetic energy of the photoelectrons, and the monolayer is defined as mentioned above, i.e. the cube edge length of the average volume occupied by titanium atoms in the layer. Thus, the resulting value obtained is λ_0 (Ti2p) = 1.21 nm (790 eV). I_0 is the intensity of Ti 2p photoelectrons which originated from the film, I_s is the intensity of Al 2p from the substrate, S_s and S_0 refer to the sensitivity factors of the substrate (Al 2p) and the film (Ti 2p), respectively. The parameters n_s and n_0 are the number of substrate and film atoms (of aluminium and titanium) per unit volume, respectively. According to the above treatment, Equation 2 may be used to determine the film thickness from the experimentally determined parameters I_0 and I_s. The XPS was employed to obtain chemical information about the Ti/Al_2O_3 interface, and the Al 2p core-level photoemission spectra collected for different coverages of titanium are presented in Fig. 4a, these coverages correspond to the equivalent thickness of 1.04, 1.36, 2.32, 3.65 and 7.64 ML. With increasing coverage of titanium, a peak at the low binding-energy side gradually develops until a shift appears in the binding energy of 2.1 eV from the Al^{3+} peak (74.8 eV), indicating the presence of reduced species, Al^0. Comparing the Al 2p lines obtained with different coverages of titanium, it is evident that the peak shapes gradually broaden. This broadening might include a contribution from some lower reduced states, $Al^{+3-\delta}$ ($\delta = 1$, 2 or 3). Up to metallic aluminium, Al^0 appeared at 72.7 eV (see Fig. 4b). It is expected that Al^{3+} in the Ti/Al_2O_3 interface was partially reduced to Al° due to a strong tendency to form Ti–O bonds at the interface. That is, titanium transfers its electrons to Al^{3+} via O^{2-} anions in the Al–O bonds, and forms stronger Ti–O bonding at the interface. Because the Al–O and the Ti–O bond strengths are similar (usually, we take the free energy of formation of metal oxide as a deciding factor), the final species at the Ti/Al_2O_3 interface will depend on

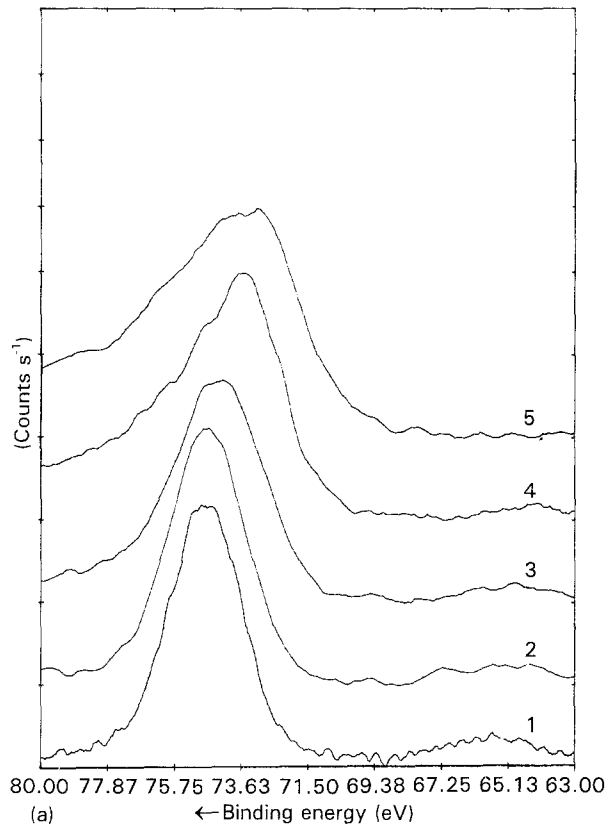

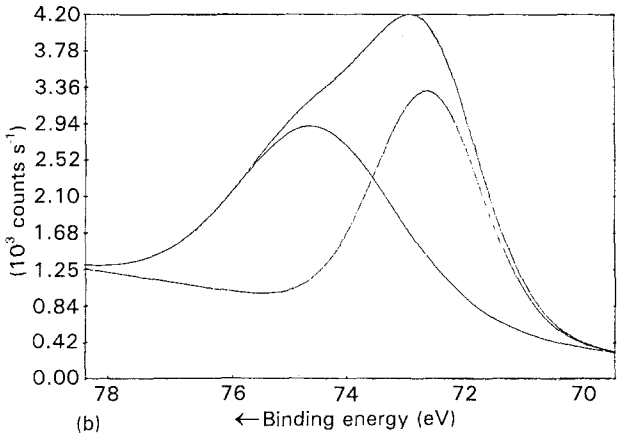

Figure 4 (a) Al 2p photoemission peaks for titanium deposited on the Al_2O_3 (1 $\bar{1}$ 0 2) plane at room temperature. The coverages are: (1) 1.04 ML, (2) 1.36 ML, (3) 2.32 ML, (4) 3.65 ML and (5) 7.64 ML. (b) The result determined by curve-fitting the Al 2p line 5 with two Gaussian–Lorentzian functions.

the chemical potential of oxygen in the titanium environment adjacent to the interface. Fig. 5 shows O 1s lines obtained for different coverages of titanium. It is clear that with increasing coverage of titanium, the chemical shift of the O 1s peak energy is about 3.0 eV from 531.5 eV, and the shape of the peaks of O 1s is broadened. A new component appeared at the low binding-energy side (528.5 eV); it implies that oxygen exists in the Ti–O form in titanium layers. Fig. 6a shows Ti 2p photoemission spectra obtained from different coverages of titanium on the Al_2O_3 (1 $\bar{1}$ 0 2) surface. There is a tendency for the shape of the Ti $2p_{3/2}$ peak on the low binding energy side to narrow progressively with increasing coverage and simultaneous shift of this peak from a binding energy of 458.4 eV to

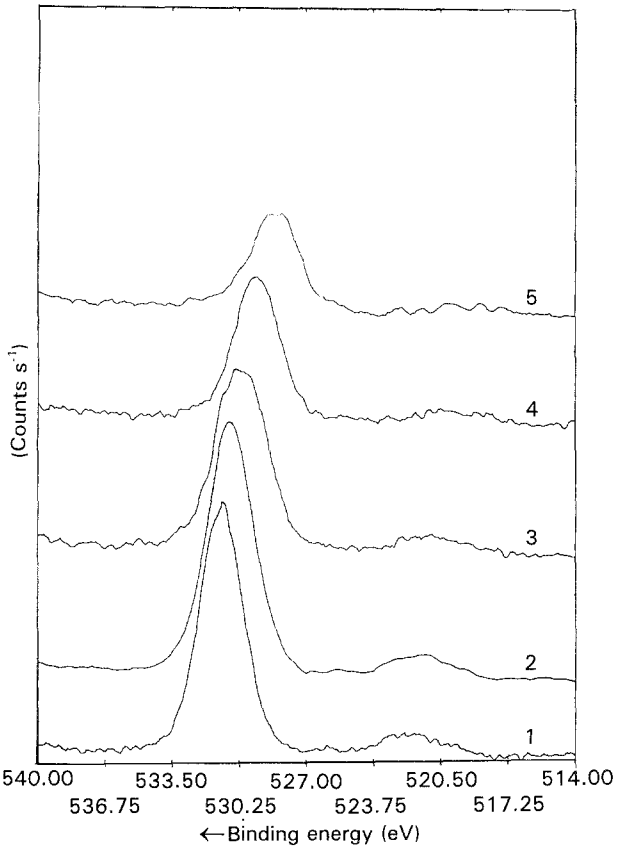

Figure 5 O 1s core-level photoemission spectra obtained with different coverages of titanium: (1) 1.04 ML, (2) 1.36 ML, (3) 2.32 ML, (4) 3.65 ML and (5) 7.64 ML.

as low as about 453.2 eV. It suggests that in the first several monolayers of titanium deposited on Al_2O_3 (1 $\bar{1}$ 0 2) surface there is an oxidized titanium. By deconvoluting the combined Ti, 2p peak obtained from the first monolayer into individual components (see Fig. 6b), it is believed that the high Ti $2p_{3/2}$ binding energy (456.4 eV) is due to TiO_2, while the lower binding energy (45.8 eV) corresponds to Ti_2O_3. This result shows that the titanium evaporated on the Al_2O_3 (1 $\bar{1}$ 0 2) surface is easily oxidized to TiO_2 or titanium-rich oxides (TiO or Ti_2O_3) due to the active oxygen anions on the surface. When the coverage of titanium is over 7.0 ML, the peak of titanium appeared at a binding energy of 453.2 eV. The AES depth profile was sensitive to aluminium, titanium and oxygen distributions. A typical Auger electron intensity profile of the Ti/Al_2O_3 system is shown in Fig. 7. Where the titanium film was grown at room temperature and at a film growth rate of 15 nm min^{-1}, growth continued until the titanium layer was about 100 nm thick. The sputtering rate was about 2 nm min^{-1}. In the AES analysis, the carbon level was very low, and the same in titanium and in Al_2O_3, suggesting that it is a background signal from the AES vacuum system. The profile of the titanium bond on the Al_2O_3 substrate gradually decreased towards the interface as cumulative sputtering time increased; simultaneously, the profile of the Al(O) which is contained in Al_2O_3 increased slowly. However, in the profile of oxygen, a high concentration region of oxygen can be seen clearly. When titanium was deposited on to an RT Al_2O_3 surface in UHV, a fraction of the first layer

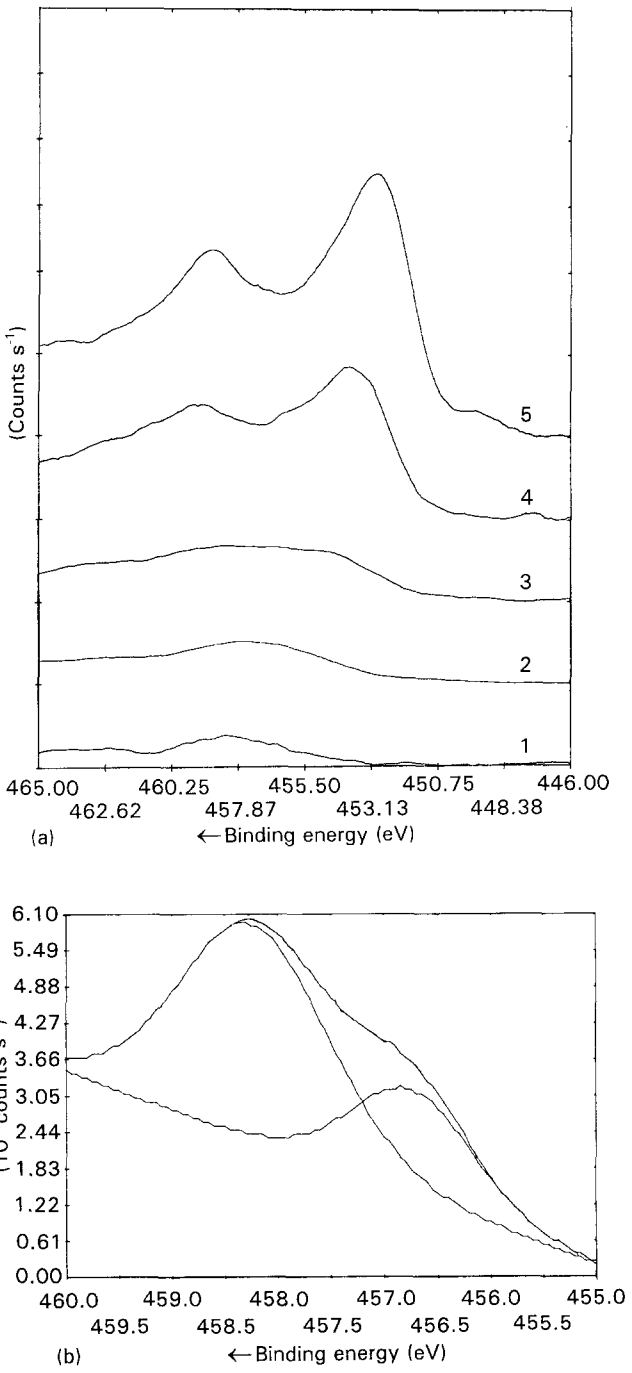

Figure 6 (a) Ti 2p photoemission spectra obtained from different coverages of titanium on the Al_2O_3 ($1\bar{1}02$) surface: (1) 1.04 ML, (2) 1.36 ML, (3) 2.32 ML, (4) 3.65 ML and (5) 7.64 ML. (b) The result determined by curve fitting the Ti 2p line 1 with two Gaussian–Lorentzian functions.

was oxidized to TiO_2 due to the active oxygen anions on the surface. Therefore, the AES profile exhibited a transient region of about 20 nm indicating the results of interaction during formation of the interface. It can be seen from Fig. 7 that an obvious reaction occurs at the Ti/Al_2O_3 interface, and the partially reduced species, Al^0, was detected by AES analysis. The formation of the high concentration region of oxygen in the interface can be explained by the defect chemistry of titanium ions in an Al_2O_3 lattice. Tetravalent Ti^{4+} ions which formed by oxidization of the active oxygen occupying trivalent Al^{3+} sites in the Al_2O_3 lattice are some point defects with positive charge. These have to be compensated by some negative charges, which are oxygen anions. Therefore, the higher the concentration of diffused titanium ions in the Al_2O_3 lattice, the greater is the number of oxygen anions which result in the increase of oxygen in this region. With increasing coverage of titanium, however, the active oxygen anions on the surface were evidently deficient. In this case, titanium ions are in the lower valence state, so they most likely cause some oxygen vacancies, resulting in a reduced active oxygen concentration. Lower oxygen activity at the surface implies lower interfacial free energy which is favourable for the interfacial reaction. In our AES profile analysis, a very thin high-resistance layer (< 1 nm) which might have a greater charging effect than that in the substrate insulator, was detected at the interface region. We suggest that it is due to the formation of a new complex oxide Ti–O–Al by oxide–oxide interaction, i.e. the original Ti/Al_2O_3 interface was replaced gradually by the titanium oxide/Al_2O_3 interface. Different reactivity of the various metals towards the surface oxygen appears to be a decisive factor governing the interaction between the metal titanium layer and the Al_2O_3 surface. The chemical reactivity of titanium with Al_2O_3 is often discussed, based on thermodynamic considerations. Interfacial reaction can usually be predicted by the standard free energy of formation change, ΔF_f, in its bulk form (see [25]). It is postulated that if the titanium atoms can establish chemical bonds directly with the oxygen anions at the Al_2O_3 surface, the strength of the bond would be directly related to the free energy of formation of Ti–O, and a high free energy implies strong chemical bonds and a strong interface. According to a hypothetical reaction

$$Ti + xAl_2O_3 \rightarrow Ti(O)_{3x} + 2x\,Al \qquad (5)$$

where (O) represents active oxygen dissolved in titanium. The driving force of the reaction in Equation 5 is the difference in the partial molar free energy of oxygen dissolved in titanium, $\Delta\bar{F}_o$, and the standard free energy of Al_2O_3 formation, ΔF_f^0. From calculations [26], this free-energy difference vanishes for an oxygen concentration of approximately 20 at %, because the free energy of formation of Al_2O_3 ($\Delta F_f^0 = -378.2$ Kcal mol^{-1}) is analogous to that of titanium oxides except a species of Ti_3O_5 ($\Delta F_f^0 = -550$ Kcal mol^{-1}). Therefore, in the view of thermodynamics, it is not always favourable to reduce Al_2O_3 directly by titanium. Thus, deciding the reactivity with the change of the free energy of formation alone is not enough. In this case, perhaps, the reaction which occurred at the interface is controlled by the system kinetics, although the nature and the process of these controlling kinetics at room temperature are still unclear to us. Assuming that the reduction of Al_2O_3 by titanium obeys the reaction of Equation 5, the velocity of the reaction would be rapid at the early stage of the interface formation, and would decrease as the oxygen concentration in the titanium layer increased. The nascent oxygen, which is generated at the Ti/Al_2O_3 interface, diffuses through the titanium layer. Therefore, obviously no metallic titanium can reach the substrate surface during the evaporation process in

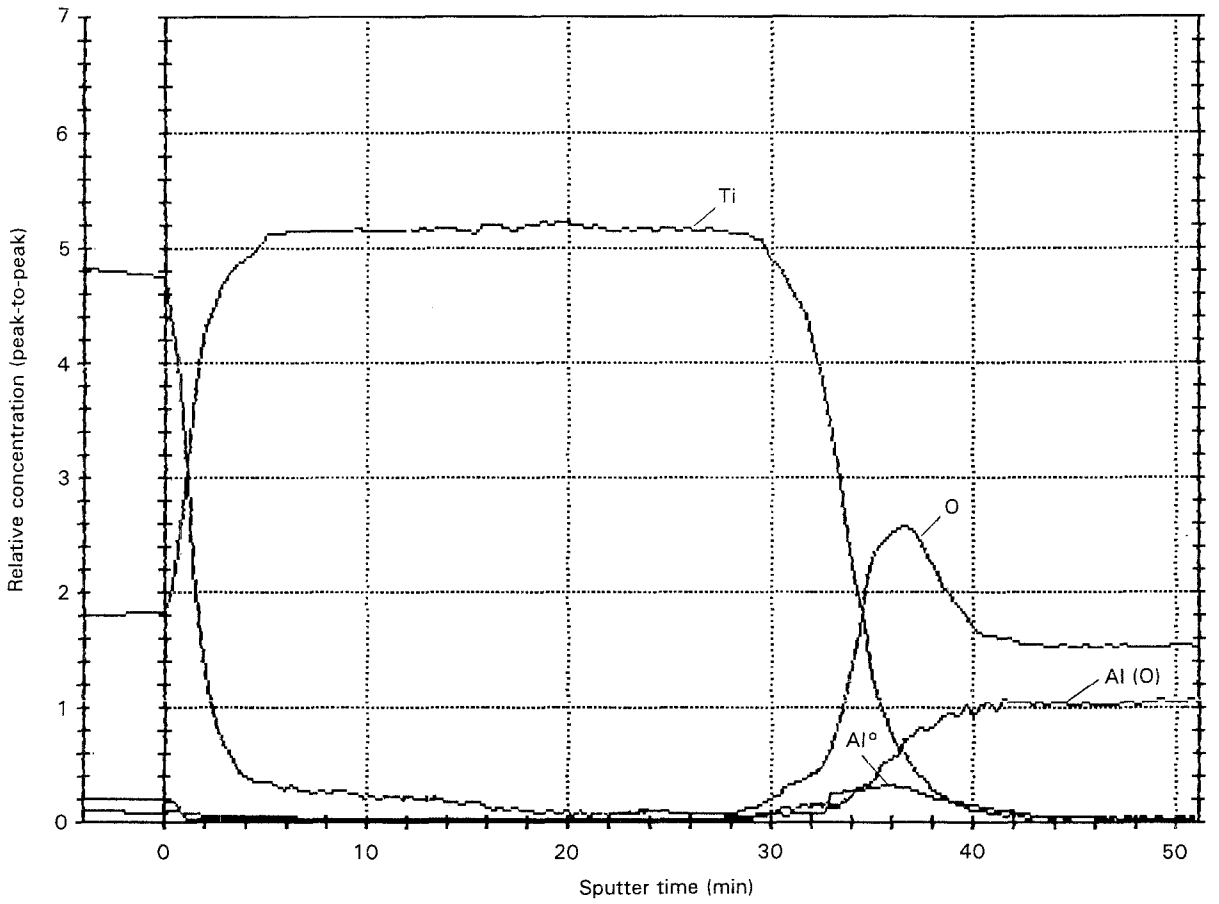

Figure 7 Auger electron depth profile of the metallized Al_2O_3 (1 $\bar{1}$ 0 2) plane after depositing titanium. The sputtering rate was 2 nm min^{-1}. The symbols Al (O) and Al^0 show the aluminium in Al_2O_3 and in the metallic state, respectively.

order to reduce the Al_2O_3. Instead, titanium oxides react with Al_2O_3 to form a complex compound which is tentatively written (Ti, Al)$_2O_3$. This suggests that the reaction layer consists of a multiphasic mixture: the Ti–O type phase, the (Ti, Al)$_2O_3$ phase and metallic aluminium phase. In fact, the metallic aluminium formed by reduction of titanium can be seen clearly in the AES profile of the Ti/Al_2O_3 system, indicating that the result of the AES analysis is consistent with that of the XPS analysis. Of course, it is also important that the environment in which a metal–sapphire bond is established can exert a great influence on the bond strength. Such small amounts of oxygen (in residual gas) in the evaporation process have probably contributed to the interface that provides enhanced bonding for active metallic titanium particularly, because, as mentioned above, the oxide–oxide interaction is stronger for the formation of the chemical bond at the interface.

4. Conclusion

We have studied the initial stages of Ti/Al_2O_3 (1 $\bar{1}$ 0 2) interface formation in ultrahigh vacuum with the aid of XPS and AES. The results show that at room temperature, a clean Al_2O_3 (1 $\bar{1}$ 0 2) surface is an aluminium-rich surface. Before and after sputtering by Ar^+ ions, the shape of the Al 2p peak, which appears to be a single peak, is unchanged, indicating the Al_2O_3 (1 $\bar{1}$ 0 2) surface is very stable. When active metallic titanium was evaporated on to a room-temperature Al_2O_3 (1 $\bar{1}$ 0 2) surface in UHV, a Ti/Al_2O_3 interface with strong adhesion was formed. With increasing coverage of titanium, the Al 2p peak shape widened, due to the formation of various reducing states of aluminium, $Al^{3+-\delta}$, up to a new peak located at a binding energy of 72.7 eV, indicating that in the interface formation, titanium transferred its electrons to Al^{3+} via O^{2-} anions in the Al–O bond and formed a Ti–O bond; thereby the Al^{3+} was reduced to metallic aluminium. The O 1s photoemission line has a greater energy shift towards the direction of lower binding energy from 531.5 eV to 528.5 eV, implying that the oxygen exists as Ti–O form in the interfacial layer. From Ti 2p spectra, we also found that in the first several monolayers of titanium deposited on the Al_2O_3 (1 $\bar{1}$ 0 2) surface there is oxidized titanium due to active oxygen anions on the surface. These results showed that the titanium films have reacted with the Al_2O_3 (1 $\bar{1}$ 0 2) surface to form titanium oxides, and the reaction correlates with the oxygen activity on the Al_2O_3 (1 $\bar{1}$ 0 2) surface. Therefore, in the light of the effect of oxygen, we suggest that the enhancement of the interfacial chemical bond and the formation of the Ti–O–Al complex oxide are due to the stronger titanium oxides–Al_2O_3 interfacial interaction. Thus, the reaction layer ought to be considered as multiphasic mixture: the Ti–O type phase, the (Ti, Al)$_2O_3$ phase and metallic aluminium phase. The Auger electron intensity profile exhibited a transient region of about 20 nm, in which the metallic aluminium reduced by titanium was detected, indicating a chemical reaction

occurs during the formation of the interface, even at room temperature. The increase of oxygen at the interface near the Al_2O_3 substrate side can be explained by the defect chemistry of the titanium ions in the Al_2O_3 lattice. For the Ti/Al_2O_3 system, the interaction occurring at the interface may be controlled by the system kinetics. It is, perhaps, more important when the difference of the free energy of formation of two metal oxides is negligible.

Acknowledgements

This work was supported by National Natural Science Foundation of China, no. 69391203. The authors are grateful to Professor Y. X. Wang for supplying the sapphire sample and for fruitful discussions.

References

1. E. A. GIESS, K.-N. TU and D. R. UHLMANN (eds), "Electronic packaging materials science", MRS Symposium Proceedings Vol. 40 (Materials Research Society, Pittsburgh, PA, 1985).
2. J. M. GIBSON and L. R. DAWSON (eds), "Layered structures, Epitaxy and Interfaces", MRS Symposium Proceedings, Vol. 37 (Materials Research Society, Pittsburgh, PA, 1985).
3. M. RUHLE, R. W. BALLUFFI, H. FISCHMEISTER and S. L. SASS (eds), *J. Phys. Colloq.* **46** (1985) C4.
4. R. E. TRESSLER, T. L. MOORE and R. L. CRANE, *J. Mater. Sci.* **8** (1973) 151.
5. M. B. CHAMBERLAIN, *J. Vac. Sci. Technol.* **15** (1978) 240.
6. J. H. SELVERIAN, M. BORTZ, F. S. OHUCHI and M. R. NOTIS, *Mater. Res. Soc. Symp. Proc.* **108** (1988) 107.
7. R. PEDDADA, K. SENGUPTA, I. M. ROBERTSON and H. K. BIRNBAUM, in "Metal-ceramic interfaces", Acta Scripta Metallurgica Proceedings Series Volume 4, edited by M. Ruhle, A. G. Evans, M. F. Ashby and J. P. Hirth (Pergamon Press, New York, 1990) p. 115.
8. Y. S. CHANG, Y. H. KIM and N. J. CHOU, *J. Vac. Sci. Technol.* **A6** (1988) 1017.
9. X. L. LI, R. HILLEL, F. TEYSSANDIER, S. K. CHOI and F. J. J. VAN LOO, *Acta Metall. Mater.* **40** (1992) 3149.
10. S. KANG and J. H. SELVERIAN, *J. Mater. Sci.* **27** (1992) 4536.
11. K. TAKAHASHI, H. ISHII, Y. TAKAHASHI and K. NISHIGUCHI, *Thin Solid Films* **216** (1992) 239.
12. *Idem, ibid.* **221** (1992) 98.
13. W. B. CARTER and M. V. PAPAGEORGE, *J. Vac. Sci. Technol.* **A10** (1992) 3460.
14. S. VARMA, G. S. CHOTTINER and M. ARBAB, *ibid.* **A10** (1992) 2857.
15. W. P. DIANIS and J. E. LESTER, *Anal. Chem.* **45** (1973) 1416.
16. W. E. SWARTZ, P. H. WATTS, J. C. WATTS, J. W. BRASCH and E. R. LIPPINCOTT, *ibid.* **44** (1972) 2001.
17. S. KOHIKI, T. OHMURA and K. KUSAO, *J. Electron Spectrosc.* **28** (1983) 229.
18. C. D. WAGNER, W. M. RIGGS, L. E. DAVIS and J. R. MOULDER, in "Handbook of X-ray photoelectron spectroscopy", edited by G. E. Muilenberg (Perkin–Elmer Co, Minnesota, 1979) p. 42, 50.
19. T. M. FRENCH and G. A. SOMORJAI, *J. Phys. Chem.* **74** (1970) 2489.
20. L. BRAGG and G. F. CLARINGBULL, "Crystal structures of minerals. The crystalline state". Vol. 4 (Bell, London, 1965).
21. M. P. SEAH and W. A. DENCH, *Surf. Interface Anal.* **1** (1979) 2.
22. Y. M. CROSS and J. DEWING, *ibid.* **1** (1979) 26.
23. S. VARMA, G. S. CHOTTINER and M. ARBAB, *J. Vac. Sci. Technol.* **A10** (1992) 2857.
24. M. J. DREILING, *Surf. Sci.* **71** (1978) 231.
25. JOHN A. DEAN (ed.) "Lange's Handbook of Chemistry", 11th edn (McGraw-Hill, New York, 1973) Sect. 9, p. 4, 57.
26. R. E. TRESSLER, in "Composite materials: Interfaces in metal matrix composites" Vol. 1, p. 285, edited by A. G. Metcalfe (Academic, New York, 1974).

Received 15 December 1993
and accepted 9 June 1994